An Improved Weighted Average Reprojection Image Denoising Method

Halimah Alsurayhi and Mahmoud R. El-Sakka(✉)

Western University, 1151 Richmond Street, London, ON N6A 3K7, Canada
halsuray@uwo.ca, elsakka@csd.uwo.ca

Abstract. Patch-based denoising algorithms have an effective improvement in the image denoising domain. Weighted Average (WAV) reprojection algorithm is a simple and effective patch-based spatial domain denoising algorithm. In this paper, an improved WAV reprojection algorithm is proposed. It improves the method by adaptively deciding the patch sizes to be used based on the image structure. The image structure is identified using a classification method based on the structure tensor matrix. The classification result is also utilized to improve the identification of similar patches in the image. The experimental results show that the denoising performance of the proposed method is better than that of the original WAV reprojection algorithm.

Keywords: Denoising · Patch-based · Weighted Average (WAV) reprojection algorithm · Structure tensor · Classification

1 Introduction

Image denoising is an important process to restore the original image signals from the noisy ones. The main objective in image denoising is to reduce noise while preserving edges and textures.

Recently, patch-based denoising algorithms have become extremely popular in the denoising field. They take the advantage of the similarity within the images, where image signals are restored by performing averaging between the similar patches in the image. Buades et al. [1] have introduced a patch based algorithm called Non-Local Means (NLM) for image denoising.

Variants of NLM algorithm have been proposed to improve its performance by adaptively selecting some of the internal parameters. Some of these variants have assigned the smoothing parameter adaptively based on the image structure [2,10,12], or based on the noise level [14]. Some other variants are based on selecting the patch size adaptively using the image structure [4,7,13]. Beside the adaptive patch size, Deledalle et al. [3] proposed a shape adaptive patches to address the problem of the halo of noise around the edges. Some other variants have improved the NLM algorithm by improving the method of computing the similarity between patches [5,8,11].

F. Karray et al. (Eds.): ICIAR 2019, LNCS 11662, pp. 207–215, 2019.
https://doi.org/10.1007/978-3-030-27202-9_18

One of the significant improvements in the patch-based denoising methods is the WAV reprojection algorithm [9] which has moved the reprojection method from the patch space to pixel space.

In this paper, we propose to improve the WAV reprojection algorithm by adaptively selecting the patch size based on the image structure. We used the structure tensor matrix to classify the image into three regions. In addition, we used the classification results to improve identifying similar patches.

This paper is organized as follow, Sect. 2 presents an explanation of the WAV reprojection algorithm and the proposed method to improve it. Section 3 demonstrates some of the experimental results. The conclusion is drawn in Sect. 4.

2 Methodology

In the WAV algorithm, the denoising is performed in three basic steps: (1) groping similar patches, (2) performing the denoising for each patch, and (3) reprojecting the denoised patches to the pixel domain (Fig. 1).

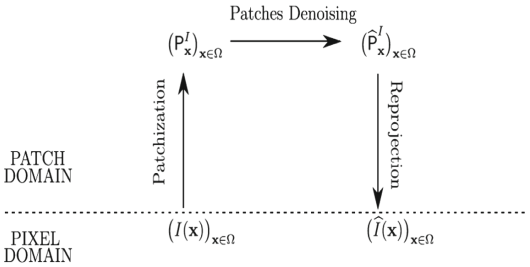

Fig. 1. The three basic steps of the WAV algorithm [9]

In the first step, similar patches are identified based on the Euclidean distance between image patches. To estimate a pixel x, a weighted average of various estimations of x is calculated as follow:

$$\hat{I}_{Wav}(x) = \sum_{i=1}^{W^2} \beta_i \hat{P}_i (W^2 - i + 1) \tag{1}$$

The weight β_i is based on minimizing the variance between patches. Because the WAV reprojection algorithm uses the flat kernel, β_i is proportional to the number of patches used to estimate $\hat{P}_i$, and $\sum_{i=1}^{W^2} \beta_i = 1$.

In the last step of the WAV reprojection algorithm, the denoised patches are reprojected to the pixel domain.

Note that, in the original NLM algorithm, only the central pixel in each patch is used to estimate the current processed pixel [1], which degrades the performance of the denoising and creates the halo of noise around the edges.

The WAV reprojection algorithm takes the advantage of the whole patch, i.e., all pixels in the patch are exploited, which enhances the denoising performance.

Edges are preserved better with a small patch size while smooth regions have better denoising performance with large patch size [12,13]. In the WAV reprojection algorithm, the patch size has set to be fixed regardless of the image structure. So, we propose an *adaptive* patch size WAV reprojection algorithm that is based on the image structure.

We used the two eignvalues of the structure tensor matrix [6] to classify the image pixels. The structure tensor matrix is defined as follow:

$$T_\sigma = \begin{bmatrix} j_{11} & j_{12} \\ j_{21} & j_{22} \end{bmatrix} = \begin{bmatrix} G_\sigma * (g_x(i,j))^2 & G_\sigma * g_x(i,j)g_y(i,j) \\ G_\sigma * g_y(i,j)g_x(i,j) & G_\sigma * (g_y(i,j))^2 \end{bmatrix} \tag{2}$$

where g_x and g_y are the gradient information in x and y directions, and G_σ is the Gaussian kernel. Then, the two eigenvalues are calculated:

$$\lambda_1 = \frac{1}{2}\left(j_{11} + j_{22} + \sqrt{(j_{11} - j_{22})^2 + 4j_{12}^2}\right) \tag{3}$$

$$\lambda_2 = \frac{1}{2}\left(j_{11} + j_{22} - \sqrt{(j_{11} - j_{22})^2 + 4j_{12}^2}\right) \tag{4}$$

where $j_{11} = G_\sigma * (g_x(i,j))^2$, $j_{22} = G_\sigma * (g_y(i,j))^2$, and $j_{12} = G_\sigma * g_x(i,j)g_y(i,j)$. We follow the classification methods provided by [12,13] to classify the image into three regions. The absolute difference between the two eigenvalues λ_1 and λ_2 is then calculated.

$$\lambda = |\lambda_1 - \lambda_2| \tag{5}$$

Then, the following classification scheme is used to classify image pixels:

$$(i,j) \in \begin{cases} c_1 & \lambda(i,j) \leq \lambda_2 \frac{(\lambda_1 - \lambda_2)}{n} \\ c_2 & \lambda(i,j) \leq \lambda_2 \frac{2(\lambda_1 - \lambda_2)}{n} \\ .. & \\ c_n & \lambda(i,j) \leq \lambda_2 \frac{n(\lambda_1 - \lambda_2)}{n} \end{cases} \tag{6}$$

This classification is inaccurate, as some pixels may belong to more than one class. So, we combined it with the discontinuity indicator provided by [12]. The discontinuity indicator classify image pixels into smooth, edge and noise. If $\lambda(i,j)$ is large, the pixel is considered to be on edge. If $\lambda(i,j)$ is small and the two eigenvalues are also small, the pixel is considered to be on smooth region. The pixel is noise if $\lambda(i,j)$ is small but the two eigenvalues are large.

In our method, we classify the image pixels into three classes based on a comparison that made upon the two eigenvalues of the structure tensor matrix. We compare the two eigenvalues of each pixel in each resulted class from Eq. 6 with a specified *threshold* value. If the two eigenvalues are smaller than the *threshold*, the pixel is considered to be in a smooth area. If the maximum eigenvalue λ_1 is larger than the *threshold* and the minimum eigenvalue λ_2 is smaller than the

threshold, the pixel is considered on edge. The pixel is on texture or a noise if the two eigenvalues are larger than the *threshold*.

$$(i,j) \in \begin{cases} Smooth & \lambda_1 < \tau,\ \lambda_2 < \tau \\ Edge & \lambda_1 > \tau,\ \lambda_2 < \tau \\ Texture/Noise & \lambda_1 > \tau,\ \lambda_2 > \tau \end{cases} \tag{7}$$

where τ is the threshold value, and it has set to be 40.

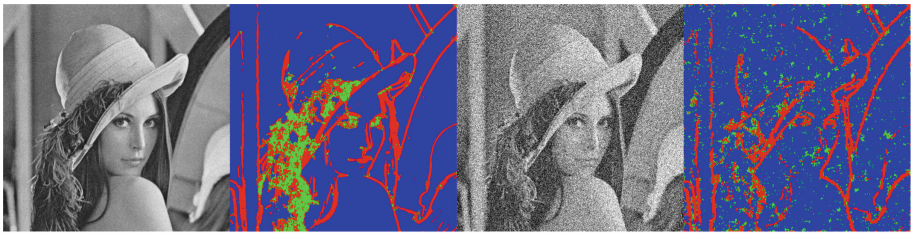

(a) (b) (c) (d)

Fig. 2. The improved classification results on Lena image. (a) noisy image with noise $\sigma = 10$, (b) its classification result, (c) noisy image with noise $\sigma = 60$, (d) its classification result (Color figure online)

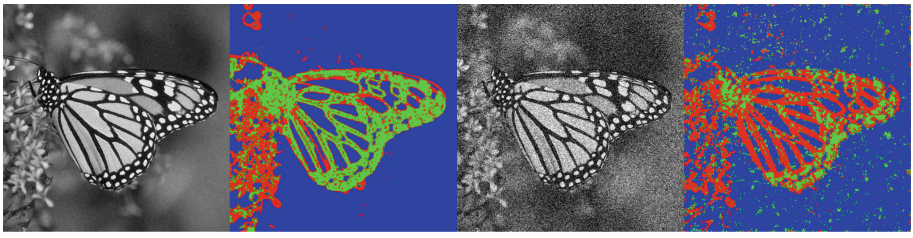

(a) (b) (c) (d)

Fig. 3. The improved classification results on butterfly image. (a) noisy image with noise $\sigma = 10$, (b) its classification result, (c) noisy image with noise $\sigma = 60$, (d) its classification result (Color figure online)

In addition, we apply a preprocessing step to improve the classification results. The image is denoised first using the original WAV reprojection algorithm. This step has improved the classification result especially at the low noise levels. The texture areas can be classified as a third class when the noise level is less than or equal to 30. However, when the noise level is high, the third class represents the noise. The resulted classifications are shown in Figs. 2 and 3 for Lena and Butterfly images, respectively, with two different noise levels ($\sigma = 10$ and $\sigma = 60$). The blue color presents the smooth areas, the red color presents the

edges, and the green color presents the texture or noise areas. When the noise level is low ($\sigma = 10$), the green color shows the texture only. While texture and noise are presented in green color when noise level is high ($\sigma = 60$). The resulted classification is then used as a mask on the noisy image. In the patchization step, patches similar to the reference patch contribute into the averaging process only if their central pixels belong to the same class. That decreases the number of un-similar patches from contributing in the averaging process.

In addition, an adaptive patch size is assigned to each pixel based on the class the pixel is belong to. A large patch size is assigned to pixels on smooth areas, and a small patch size is assigned to pixels on edges. For the texture, a smaller patch size is assigned. Figure 4 shows the block diagram of the proposed scheme. The next section explains the experimental results used to assign the best patch size for each class.

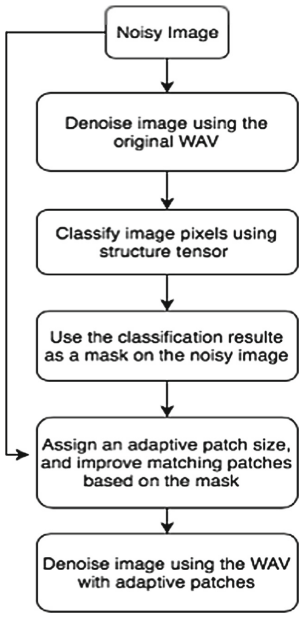

Fig. 4. The basic steps of our improved method

3 Experimental Results

We compared the performance of our adaptive WAV reprojection method with the original WAV algorithm. The restored images are compared in term of the peak signal-to-noise ratio (PSNR), and the visual quality. The PSNR is defined as:

$$PSNR = 10 \ \log_{10}\left(\frac{(MAX)^2}{MSE}\right) \tag{8}$$

where MSE is *Mean Squared Error* between the original image corrupted image, MAX is the maximum pixel intensity value. In our experiments, we targeted the natural scene images. We used 25 images. The images are contaminated by additive white Gaussian noise with various levels of noise to assess the performance of each class at each noise level and when using different patch sizes.

Table 1. The mean PSNR values of smooth areas in 25 different natural scene images using 10 different noise levels

Noise level	5×5	7×7	9×9	11×11	13×13
10	37.16	37.27	**37.31**	37.21	37.00
20	33.12	33.28	33.35	**33.36**	33.32
30	30.74	30.96	31.03	**31.04**	31.02
40	29.13	29.40	29.48	**29.50**	29.49
50	27.86	28.19	28.28	**28.30**	28.30
60	26.90	27.28	27.39	**27.41**	27.40
70	26.14	26.58	26.70	**26.72**	**26.72**
80	25.48	25.95	26.07	**26.10**	**26.10**
90	24.90	25.40	25.53	**25.56**	**25.56**
100	24.34	24.88	25.03	**25.06**	**25.06**
Mean	28.58	28.92	29.02	**29.03**	29.00

Tables 1, 2 and 3 show the resulted mean PSNR values for smooth, edges and texture/noise areas respectively. The patch size 11×11 have the best mean PSNR value in smooth areas. Pixels on edges have the best results when patch size of 7×7 is used. For the texture areas, patch size of 5×5 has the best mean PSNR performance. As the third class (texture) represents noise, when the noise level is more than 30, patch size of 11×11 is assigned. The patch size, $w \times w$, is selected as shown below:

$$w = \begin{cases} 11, & Smooth,\ (Texture/Noise\ (\sigma > 30)) \\ 7, & Edge \\ 5, & Texture/Noise\ (\sigma \leq 30) \end{cases} \tag{9}$$

The WAV reprojection algorithm has used a fixed patch size of 9×9 for the entire image. For the searching window size, 9×9 is used in both methods.

Our adaptive method has improved the denoising performance. It produced better PSNR values than the original WAV reprojection method. Table 4 presents the mean PSNR values for 10 images at 10 different noise levels. In addition, the edges and textures are preserved better in our adaptive method due to applying small patch sizes at the edge and texture areas. Figure 5 shows how our adaptive method has reduced the artefact around Lena's eyes. Figure 6 also shows that the artefact has been reduced with our proposed method. The PSNR performance for those areas are reported.

Table 2. The mean PSNR values of edge areas in 25 different natural scene images using 10 different noise levels

Noise level	5×5	7×7	9×9	11×11	13×13
10	**32.81**	32.62	32.22	31.85	31.58
20	28.46	**28.60**	28.54	28.34	28.11
30	25.70	**25.82**	25.77	25.64	25.46
40	23.81	**23.87**	23.78	23.63	23.44
50	22.47	**22.48**	22.37	22.21	22.02
60	21.59	**21.60**	21.48	21.32	21.14
70	20.98	**21.02**	20.93	20.79	20.64
80	20.68	**20.78**	20.72	20.61	20.49
90	20.49	**20.66**	20.64	20.56	20.47
100	20.41	20.65	**20.68**	20.64	20.57
Mean	23.74	**23.81**	23.71	23.56	23.39

Table 3. The mean PSNR values of texture areas (or noise) in 25 different natural scene images using 10 different noise levels

Noise level	5×5	7×7	9×9	11×11	13×13
10	**29.47**	29.05	28.78	28.63	28.56
20	**25.25**	24.89	24.61	24.43	24.34
30	**23.29**	23.18	23.03	22.94	22.88
40	22.37	22.44	**22.45**	22.42	22.39
50	22.33	22.53	22.61	**22.63**	22.58
60	22.67	23.00	23.13	**23.17**	23.13
70	22.92	23.32	23.49	**23.54**	23.53
80	22.94	23.39	23.56	**23.62**	23.61
90	22.79	23.29	23.47	**23.53**	23.52
100	22.47	23.02	23.22	**23.29**	**23.29**
Mean	23.65	23.81	**23.84**	23.82	23.78

Table 4. The PSNR values for 10 different natural images in 10 noise levels

Noise level	10	20	30	40	50	60	70	80	90	100
Original WAV	34.14	30.87	28.74	27.11	25.93	25.01	24.30	23.72	23.19	22.74
Proposed method	**34.37**	**31.01**	**28.96**	**27.31**	**26.20**	**25.29**	**24.58**	**23.94**	**23.34**	**22.81**

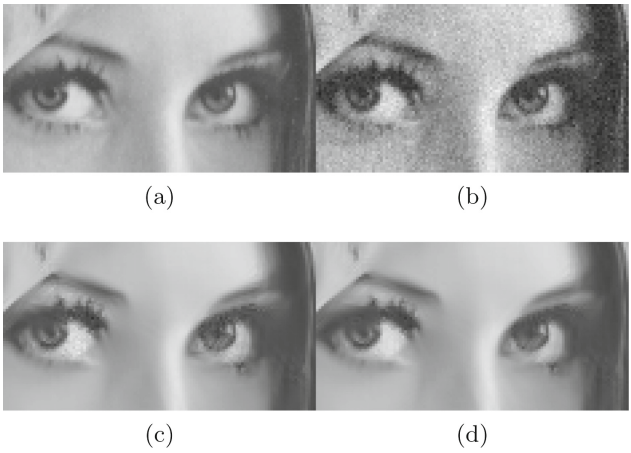

Fig. 5. A zoomed portion from Lena image denoised using the original WAV reprojection algorithm and our proposed method. (a) a portion from original Lena image, (b) noisy image with noise $\sigma = 10$ (PSNR = 23.82), (c) denoised image with the original WAV reprojection algorithm (PSNR = 34.22), (d) denoised image using our improved method (PSNR = 34.84).

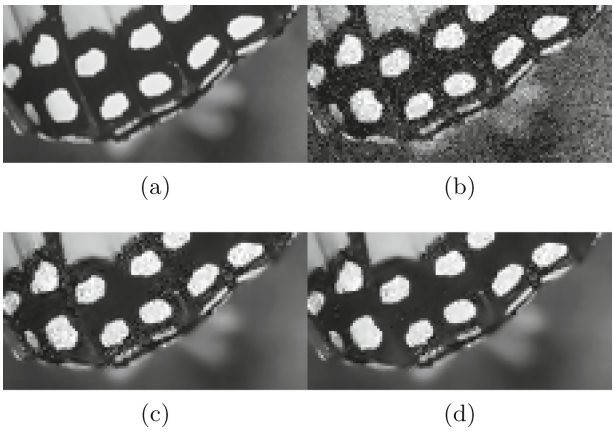

Fig. 6. A zoomed portion from butterfly image denoised using the original WAV reprojection algorithm and our proposed method. From left to right and up to bottom: a portion from original Lena image, noisy image with noise $\sigma = 20$ (PSNR = 22.47), image with the original WAV reprojection algorithm (PSNR = 25.96), denoised image using our improved method (PSNR = 26.69).

4 Conclusion

In this paper, an improved WAV reprojection algorithm is presented. The image pixels is first classified into three regions: smooth, edges, and texture (or noise). Then, an adaptive patch size is assigned for each class. In addition, grouping

similar patches has improved by the resulted classification mask. Experimental results show the improvement of our methods over the original WAV reprojection algorithm, especially around the edges.

References

1. Buades, A., et al.: A non-local algorithm for image denoising. In: IEEE Computer Society Conference on Computer Vision and Pattern Recognition, vol. 2, pp. 60–65 (2005)
2. Chen, M., Yang, P.: An adaptive non-local means image denoising model. In: 2013 6th International Congress on Image and Signal Processing (CISP), vol. 1, pp. 245–249. IEEE (2013)
3. Deledalle, C.-A., Duval, V., Salmon, J.: Non-local methods with shape-adaptive patches (NLM-SAP). J. Math. Imaging Vis. **43**(2), 103–120 (2012)
4. Hu, J., Luo, Y.-P.: Optik non-local means algorithm with adaptive patch size and bandwidth. Optik Int. J. Light Electron Opt. **124**(22), 5639–5645 (2013)
5. Hu, J., Pu, Y., Wu, X., Zhang, Y., Zhou, J.: Improved DCT-based nonlocal means filter for MR images denoising. Comput. Math. Methods Med. **2012**, 1–14 (2012)
6. Knutsson, H.: Representing local structure using tensors. In: 6th Scandinavian Conference on Image Analysis, Oulu, Finland, pp. 244–251. Linköping University Electronic Press (1989)
7. Lan, X., Shen, H., Zhang, L.: An adaptive non-local means filter based on region homogeneity. In: IEEE Seventh International Conference on Image and Graphics, pp. 50–54 (2013)
8. Peter, J.D., Ramya, R.: A novel adaptive non local means for image de-noising. Procedia Eng. **38**, 3278–3282 (2012)
9. Salmon, J., Strozecki, Y.: Patch reprojections for non-local methods. Signal Process. **92**(2), 477–489 (2012)
10. Verma, R., Pandey, R.: Grey relational analysis based adaptive smoothing parameter for non-local means image denoising. Multimed. Tools Appl. **77**(19), 25919–25940 (2018)
11. Wu, K., Zhang, X., Ding, M.: Curvelet based nonlocal means algorithm for image denoising. AEU Int. J. Electron. Commun. **68**(1), 37–43 (2014)
12. Zeng, W., Du, Y., Hu, C.: Noise suppression by discontinuity indicator controlled non-local means method. Multimed. Tools Appl. **76**(11), 13239–13253 (2017)
13. Zeng, W., Lu, X.: Region-based non-local means algorithm for noise removal. Electron. Lett. **47**(20), 1125–1127 (2011)
14. Zhu, S., Li, Y., Li, Y.: Two-stage non-local means filtering with adaptive smoothing parameter. Optik Int. J. Light Electron Opt. **125**(23), 7040–7044 (2014)